Modeling the relative power reduction factor of a PV generator installed on different piers

Abstract *- The factors causing power loss in a generator are numerous; this manuscript is dedicated to modeling and simulating the influence of trellises (-reinforced concrete, -iron, -steel, -aluminum, -sand, -earth, -gravel, -water, -seckho, -baked brick, -air, and -straw) on the power of a PV Generator (PVG). The objective is to observe the losses due to the heating of the Back Surface Field (BSF) of the PVG caused by the different types of trellises. The test is carried out over a period of 5, 10, 15, 20, and 25 years at different installation sites.The results from the MATLAB/script simulation showed that the supports on which the PV system is installed over 5 years reduce the power by: 26.36%, 25.32%, 26.97%, 22.14%, 22.62%, 23.90%, 27.60%, 24.64%, 23.80%, 27.51%, and 21.42% for the different piers. Our PV system experienced an average power loss factor of: 20.90% (5 years), 20.01% (10 years), 23.01% (15 years), 22.25% (20 years), and 21.53% (25 years). It appears that a favorable site for installing a PV system is either to suspend it at a certain height (pier-air) or to install it on water (pier-water).*

Keywords*: Modeling-Power Loss-Pier-PV System.*

Introduction

Experiments have shown that after prolonged exposure to natural climatic conditions, thermal stresses and a deterioration in the electrical performance of photovoltaic modules are observed [[1], [2], [3], [4]]. Therefore, a thorough analysis of the causes of the reduction in maximum power and the aging of PV systems is necessary. Such an analysis inevitably involves studying the degradation of the I-V curve due to the effects of the mounting structure or site-specific factors (surface: concrete, sheet metal, metal, wood, planks, seckho, sand, water, vegetation, etc.) on PV modules installed in a harsh environment.Let us recall that the metallic contacts on the emitter and the substrate serve to collect the photogenerated carrier current; the contacts must be ohmic [5]. The rear surface (full metallization) of the solar cell is characterized by a very high surface recombination velocity. The back surface electric field (Back Surface Field, BSF) involves creating a potential barrier (for example, a p+-p or n+-n junction) on the rear side to ensure passivation.The potential barrier induced by the difference in doping levels between the base and the BSF tends to confine minority carriers within the base. As a result, they are kept away from the rear surface. Therefore, the absence of an electric field at the rear surface near the ohmic contact causes the minority carriers to be drawn into the space charge region, leading to poor collection. This results in a deterioration of photocurrent, open-circuit voltage, and photovoltaic conversion efficiency [6]. This article aims to observe the modeling of power evolution of a PV system installed on different trestles. To carry out this work, we structured it

into three sections: the first section (1) presents and describes the phenomenon of trestles on the solar cell; the second section (2) covers the mathematical and material formalisms; the last section (3) presents the results and discussion [7-8].

1. Degradation of the PV module

Published data on photovoltaic (PV) degradation rates have been aggregated and re-examined. The topic has garnered increased interest in recent years, leading to over 11,000 degradation rates reported across nearly 200 studies conducted in 40 different countries. (Dirk Jordan, Sarah Kurtz, Kaitlyn VanSant, Jeff Newmiller).

1.1. Factors of cell degradation

This section describes the various rates resulting from the degradation of PV in a harsh environment. The degradation of PV modules is related to the decline in the electrical performance parameters of the modules, such as the short-circuit current, open-circuit voltage, and fill factor. These electrical performance parameters depend on the solar cell parameters, such as the reverse saturation current, the ideality factor, and parasitic resistance (series resistance and shunt resistance), which are the basis for losses in PV modules [[9] - [14]].According to Un. Bouaichi, et al. [15], high temperatures and humidity discolor the transparent ethylene-vinyl acetate (EVA) encapsulation sheet of photovoltaic modules and prevent incident photons from reaching the solar cells. This degrades the short-circuit current and the output power of PV modules [[8] - [28]].Another key factor that accelerates the degradation of photovoltaic modules is the accumulation of dust on the modules. The accumulation of dust on photovoltaic modules largely depends on the properties of the dust such as weight, shape, size, and chemical properties, as well as environmental conditions such as weather, environmental characteristics, and site-specific factors. In Iraq, M.A. Hadnan et al. 2024 [29] stated the impact of soiling losses on energy yield, revealing potential losses of up to 70%.

Furthermore, despite evidence suggesting variations in degradation rates depending on climatic conditions ([3] - [30]), photovoltaic panel manufacturers have been reluctant to implement performance degradation warranties based on the racking. This divergence highlights the need for comprehensive global assessments of the reduction rates of photovoltaic modules in order to provide manufacturers with concrete evidence of the differentiation of degradation rates related to different types of racking.

1.2. Mathematical formalism for evaluating PV degradation

1.2.1. Photovoltaic Generator (PVG)

The specific site factor (Pinst) allows for the observation of losses in a PV generator due to the effects of the structure. It is the factor that multiplies the photocurrent and affects the incident flux (generation-recombination rate) and the carrier diffusion length rates (Ln, Lp) [[3], [19]].Losses at the surface of the solar cell are modeled by surface recombination with a rate that characterizes the quality of the surfaces. The base of the solar cell consists of two regions: the actual base and a heavily doped area near the rear ohmic contact. Such a structure leads to two consequences: the creation of a small additional energy barrier and the confinement of minority carriers in the base.In this way, the charge carriers generated at the back of the base near the ohmic contact, which are normally lost in simple cells, are recovered. The loss of minority carriers at the rear surface of the solar cell is quantified by the recombination current at the surface of the rear ohmic contact; given by equation [[1] - [2]]:

$$I = \left[I_{Phref} - K_i.\left(T - T_{ref}\right)\right].\frac{\varepsilon_{fss}.G}{G_{Ref}} - I_0.\left[exp\left(\frac{(V+R_S.I)}{m.V_t}\right) - 1\right] - \frac{(V+R_S.I)}{R_P}.\left[1 + a\left(1 - \frac{(V+R_S.I)^{-n}}{V_b}\right)\right] \quad (1)$$

$$T = \left[\frac{NOCT-20}{0.8}\right].G + T_a \quad (2)$$

T: is the temperature under normal NOCT conditions

This equation describes the current flowing through the solar cell by applying Kirchhoff's law.

Note: At the MPPT (Maximum Power Point Tracking) point and under NOCT conditions, we are:

$$G = 1000\,\frac{W}{m^2}\,, T = 25°C\,, AM = 1.5\,, I_m \approx 0.8.\,I_{CC}\ \text{et}\ V_m \approx 0.8V_{CO} \quad (4)$$

Temporary degradation rate

The temporary degradation rate due to the specific site factor is given by:

$$\tau_{fss}\,(\%) = \left(1 - \frac{X_{mes}}{X_m}\right).100\ \text{et}\ \tau_{Jour} = \left(\frac{\tau_{fss}\,(\%)}{t_{expo}}\right) \quad (5)$$

1.2.2. GPV Power Losses

In this section, we explain the modeling process. We took into account:

The installation duration, the technology, the power characteristics, the specific site, and the orientation angle of the cell. We varied the site specificity (reinforced concrete, sheet metal, tile, back sheet, earth, sand, water, straw, aluminum, soil, diatomaceous earth, natron, clay, plastic, glass, vacuum) for the same PV system, then we proceeded to measure the values using a digital multimeter and a pyrometer.

2. Materials and Methods

2.1. Module & Simulation Parameters

STC module power [W]: P_STC = 300 Wc;

Temperature coefficient (°C): temp_coeff = -0.004; => -0.4%/°C => -0.004 /°C

Nominal Operating Cell Temperature [°C]: NOCT = 45;

Annual intrinsic degradation (0.5%/year): intrinsic_deg_rate = 0.005;

Simulation duration [years]: years = 5, 10, 15, 20, and 25 years;

Time step in hours: dt = 1; t_hours = 0:dt:(years*365*24 - 1); t_years = t_hours / (365*24);

Irradiance/day:

$$\text{Irradiance} = \text{hourly profile (sine)} + \text{seasonal variation} \quad (6)$$

With: Gmax = 1000 W/m^2 peak

Daily factor:

$$\text{day\_factor} = 1 + 0.2\sin(2\pi * \text{t\_years}); \quad (7)$$

Seasonal variation:

$$\text{Seasonal variation} \ +/-20 \ \text{hour\_of\_day} = \text{mod}(\text{t\_hours}, 24); \quad (8)$$

$$G = \text{Gmax} \,.\, \max(0, \sin(\text{pi} * \text{hour\_of\_day} / 12)) .* \text{day\_factor} \quad (9)$$

Ambient temperature:

Ambient temperature = seasonal variation + daily variation

Average temperature: Tamb_mean = 20 °C

Seasonal amplitude: Tamb_amp_season = 8;

Daily amplitude: Tamb_(amp_diurnal) = 5;

$$\text{Tamb} = \text{Tamb\_mean} + \text{Tamb\_amp\_season} * \sin(2\pi * \text{t\_years} - 0.5) \ldots$$

$$+ \text{Tamb\_amp\_diurnal} * \sin(\frac{2\pi * \text{hour\_of\_day}}{24}); \quad (10)$$

Table 1. Table of substrates (assumptions)

fields	
name	Name
deltaT_eff	effect of the substrate on module temperature at 1000 W/m² [°C]
soiling_rate	deposit accumulation rate (1/year)
max_soiling	maximum relative loss due to soiling (fraction)
corrosion_rate	corrosive effect in additional annual relative loss

$nSubs = length(substrates);$

Calculations for each substrate

Instantaneous power [W]

$P\_time = zeros(nSubs, length(t\_hours));$

Power relative to STC

$relPower = zeros(nSubs, length(t\_hours));$

$$\begin{cases} \text{for k = k = 1: nSubs} \\ \text{s = substrates(k);} \end{cases} \quad (11)$$

Approximate cell temperature =

$$\text{Tamb} + (\text{NOCT} - 20)/800 * \text{G} + \text{substrate effect pro rata G}/1000 \quad (12)$$

$$\text{Tcell} = \text{Tamb} + (\text{NOCT} - 20)/800 .* \text{G} + \text{s.deltaT\_eff} .* (\text{G}/1000); \quad (13)$$

Cumulative soiling over time:

$$\text{soiling\_frac(t)} = \text{max\_soiling} * \left(1 - \text{e}^{(-\text{soilin g}_{\text{rate}} * \text{t}_{\text{years}})}\right); \quad (14)$$

$$\text{soiling\_frac} = \text{s.max\_soiling} .* \left(1 - \text{e}^{(-\text{soilin g}_{\text{rate}} * \text{t}_{\text{years}})}\right); \quad (15)$$

Annual multiplicative degradation (intrinsic + corrosion), applied over time:

$$factor = e^{(t\_years * ln\ (1 - total\_rate\ ))}$$

(16)

$$total_{rate} = intrinsic_{deg_{rate}} + s * corrosion\_rate;$$

(17)

To avoid a negative base if total_rate>1, we take an approximate negative exponent:

$$\text{deg}_{factor} = e^{(-total_{rate} .* t_{years})};$$

(18)

$$e^{(-rate * t)} \approx e^{t * \ln(1 - rate)}, pourlespétitsrates \quad (19)$$

Instant power:

$$P = P\_STC * (\frac{G}{1000}) * (1 + temp\_coeff * (Tcell - 25)) * (1 - soiling\_frac) * deg\_factor$$

(20)

$$P\_inst = P\_STC .* (\frac{G}{1000})(1 + temp\_coeff .* (Tcell - 25)) .* (1 - soiling\_frac) .* deg\_factor; \quad (21)$$

Clamp negatives

$$P\_inst(P\_inst < 0) = 0; \quad (22)$$

$$P\_time(k,:) = P\_inst; \quad (23)$$

P_STC fraction

$$relPower(k,:) = P\_inst ./ P\_STC; \quad (24)$$

2.2. Equipment

The different platforms for installing a photovoltaic system.

Figure 1. Different types of photovoltaic installation racks

Matlab 2025b

Figure 2. Workstation

Computer: Surface Go I5 10th Generation N2B2UOM

3.. Results and Discussion

159 This section presents the results of our simulation

160 **3.1. Simulation of the relative power of the GPV according to different piers**

161 The figure below shows that the power is affected by the site characteristics on which a PV
162 system is installed and by its lifespan.

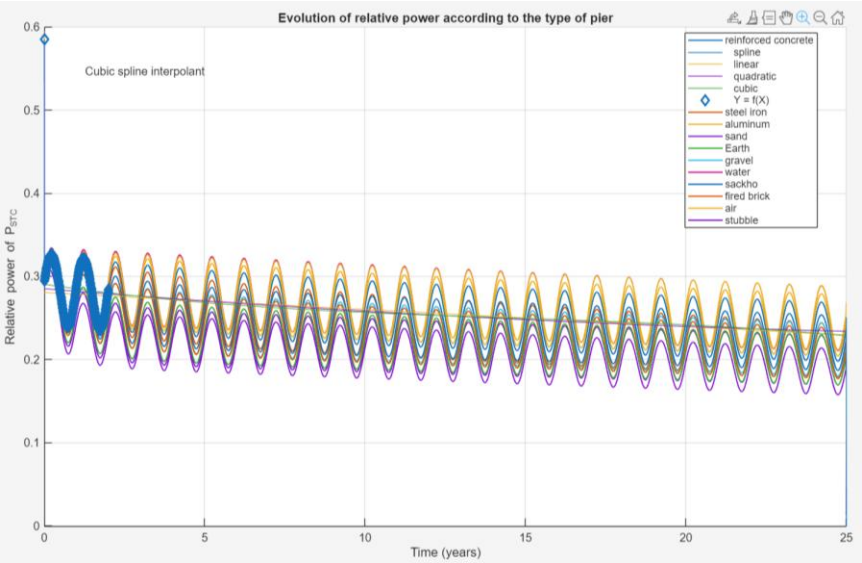

163

164 **Figure 3. Evolution of relative power according to the type of piers**

165 Figure 3 describes the influence of different piers on the relative power (PSTC). We observe that
166 with iron, aluminum, and gravel piers, the losses are more pronounced than at other sites. This
167 reduction ultimately leads to the degradation of the photovoltaic panel, which in turn causes the
168 disintegration of the associated static converters. This demonstrates that a very specific site must
169 be chosen to install PV systems; however, in sub-Saharan Africa, and especially in Chad, solar
170 panels are generally installed directly on the ground or on metal roofs. Also, it should be noted
171 that over time, the voltage drops due to the effects of piers increase, as highlighted in the figure
172 above.

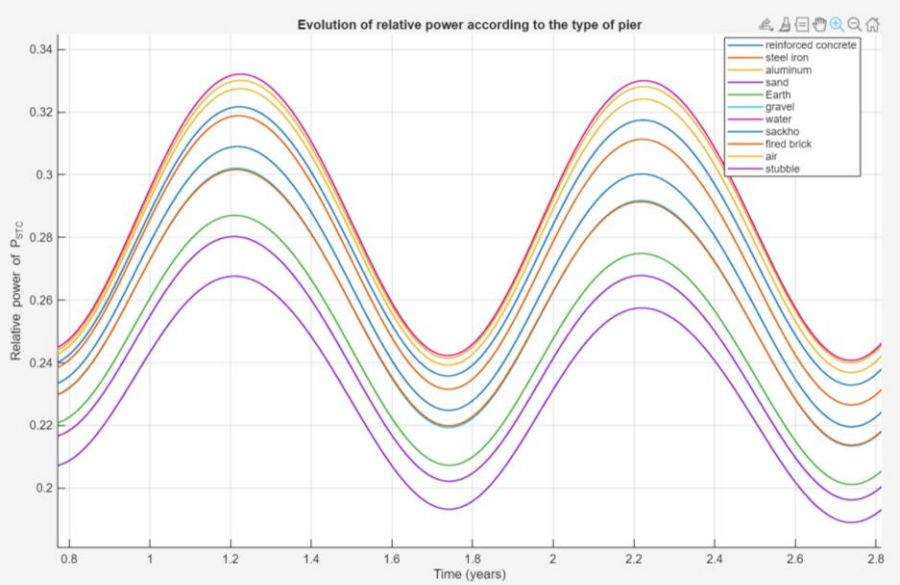

Figure 4. Zoom on the influence of different jetties

In this Figure 4, we observe that the PV system loses more of its performance when installed on sand, straw, and soil. This can be explained by the fact that the Sahelian climate, coupled with the thermoelectric properties of these sites (sand, straw, and soil), affects the performance of the PV system.

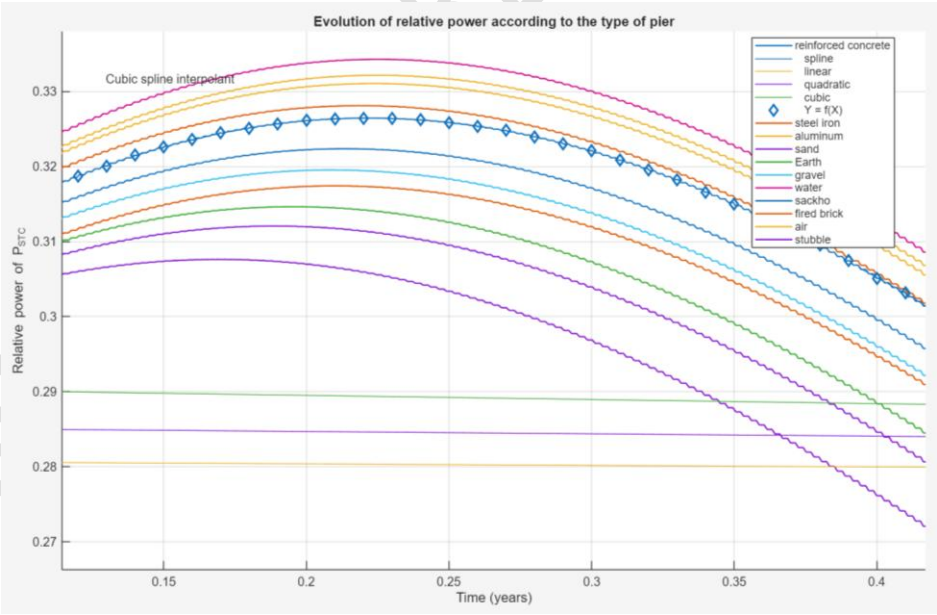

Figure 5. Acceptable range of pier areas

Figure 5 shows the range of acceptable piers for the installation of a photovoltaic generator without significant power loss. To outline these areas, we drew a line using the geometric regression law y = f(x) based on the simulated data.

Thus, this curve serves as a boundary: above it, conditions are considered favorable for optimal efficiency. Conversely, sites located below the line y = f(x) show insufficient performance and are not recommended. The position of a point relative to the line takes into account factors such as the angle of incidence, reflection, and environmental absorption. We have identified several materials and surfaces (piers) that enhance capture and minimize losses.

Reinforced concrete, for example, provides a stable and reflective surface that limits the effects of local shading. Aluminum offers good reflectivity and durability, supporting consistent performance. Fired brick combines thermal inertia with a texture suitable for long-lasting installation. Water, when present in a calm and reflective form, can increase the received irradiation through reflection. Air, understood here as open areas without obstacles, reduces losses related to shading and diffusion. Consequently, we recommend installing PV generators on these supports or in these environments when conditions allow. For sites below y = f(x), corrective measures (elevation, change of orientation, or surface treatment) are necessary before installation.

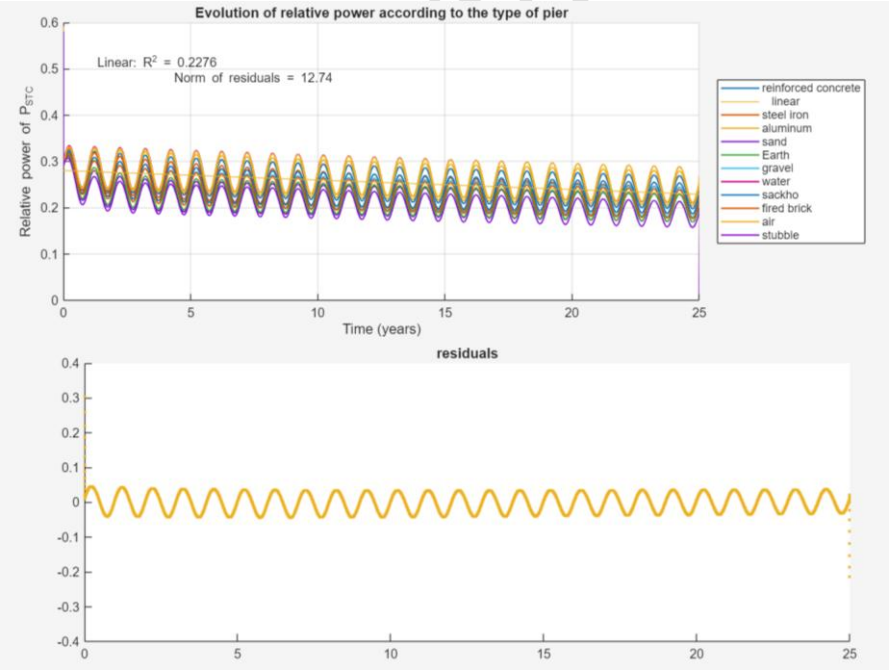

Figure 6. Range of the favorable zone over 25 years

In this figure 6, we observe that even over a period of 25 years, sites made of reinforced concrete, aluminum, air, and water have remained favorable for solar installations.

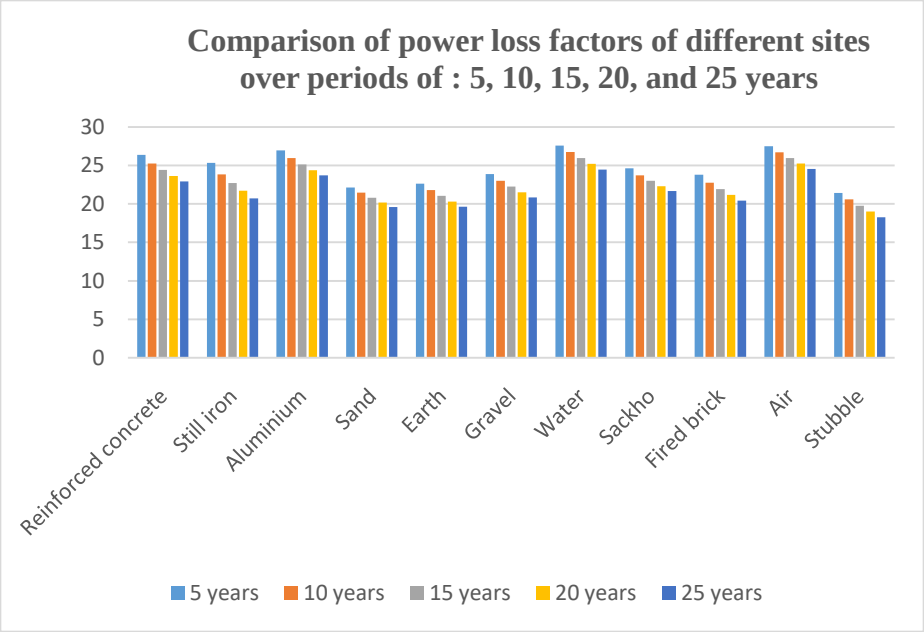

Figure 7. Comparison of power loss factors at different sites over periods of 5, 10, 15, 20, and 25 years.

Figure 7 compares the rate of reduction in GPV power across different types of piers over a period ranging from 5 to 25 years in 5-year increments. It appears that: in the case of reinforced concrete during the first period of 5 to 10 years, GPV is not significantly affected by thermo-electric factors due to the local climate. In the case of air, water, and aluminum, these materials constitute favorable piers for optimizing GPV performance.

4.. Conclusion

In this article, a simulation is conducted to observe the influence of racks on the power of a 300Wp PV system. Among the various installation sites, we found that platforms made of concrete, aluminum, air, and water remain favorable supports for BSF protection and contribute to optimizing production, whereas other sites significantly affect the efficiency of the PV system. This result explains that the installation of a PV system in households should no longer be done at random, as one of the sources of voltage drops and the degradation of photovoltaic converters is due to the racks on which the panels are mounted.

5.. References

[1] D.C. Jordan, S.R. Kurtz, K. Van Sant Newmiller. Compendium of Photovoltaic Degradation Rates Prog. Photovoltaics Res. Appl., 24 (7) (2016), p. 978-989, 10.1002/pip.2744

[2] SAKA GONI et al., (2019). Observation and Simulation of Available Solar Energy in N'Djamena, Chad, Smart Grid and Renewable Energy, 10, 165-178.

[3] H. Al-Lami, N.N. Al-Mayyahi, Q. Al-Yasiri, R. Ali, A. Alshara. Enhancement of Photovoltaic Module Performance Using a Finned Phase Change Panel: An Experimental Study in Hot Climate Conditions in Iraq, Energy Sources. (Sept. 2022), p. 6886-6897, 10.1080/15567036.2022.2103601

[4] M. Al-Damook, K. Waleed Abid, A. Mumtaz, D. Dixon-Hardy, P.J. Heggs, M. Al Qubeissi Evaluation of photovoltaic module efficiency: the case of Iraq Alex. Eng. J., 61 (8) (August 2022), pp. 6151-6168, 10.1016/j.aej.2021.11.046

[5] D. Hassan Daher, L. Gaillard, C. Ménézo Experimental evaluation of long-term performance degradation of a photovoltaic power plant operating in a desert maritime climate Renew. Energy, 187 (March 2022), pp. 44-55, 10.1016/j.renene.2022.01.056

[6] Yassin Yehia Rady, Matteo V Rocco, M.A.Serag-Eldin, Emanuela Colombo. Modeling for Power Generation Sector in Developing Countries: Case of Egypt. Energy 165September 2018 DOI:10.1016/j.energy.2018.09.089

[7] J.J. Liou et al., 'Comparison and Optimization of the Performance of Si and GaAs Solar Cells,' Solar Energy Materials and Solar Cells, Vol. 28, pp. 9 – 28, 1992;

[8] M.J. Yaseen, N.K. Kasim, A.F. Atwan Prediction of the performance of a photovoltaic solar system in Baghdad, Iraq, vol. 2322 (August 2022), article 012079, 10.1088/1742-6596/2322/1/012079;

[9] D. Atsu, I. Seres, M. Aghaei, I. Farkas Analysis of the long-term performance and reliability of photovoltaic modules under tropical climate conditions in Sub-Saharan Africa, Renewable Energy, 162 (Dec. 2020), p. 285-295, 10.1016/j.renene.2020.08.021

[10] Noël Djongyang et al., Renewable Energy in Sub-Saharan Africa, Ed. Harmattan Cameroon, 370p September 2012.

[11] Noël Djongyang et al. Food Security and Photo-Irrigation. Ed. Harmattan Cameroon, 322p, September 2019.

[12] [J. KENGNE OUABO et B. LAPONCHE, Energy Consumption in ECOWAS and CEMAC Countries, July 2011.

[13] [A. ABUBAKAR Mas'u et al., A Review on the Recent Progress Made on Solar Photovoltaics in Selected Countries of Sub-Saharan Africa. Renew. Sustain. Energy, vol. 147, Suppl. C, pp. 358-367, May 2017.

[14] M. Taraba et al. Measurement of Thin-Film Solar Panel Properties under Adverse Weather Conditions. Transp Res Procedia (2019)

[15] Un. Bouaichi, et al. In Situ Evaluation of Early Degradation of Photovoltaic Modules of Various Technologies under Harsh Climate Conditions: The Case of Morocco. Renew. Energy, 143 (Dec. 2019), pp. 1500-1518, 10.1016/j.renene.2019.05.091

[16] E.J. Schneller et al. Manufacturing Metrology for the Reliability and Durability of c-Si Modules. Renew. Sustain. Energy Rev (2016)

[17] M.B. Strobel et al. Uncertainty of photovoltaic performance parameters - dependence on location and material Sol Energy Mater Sol Cells (2009) [18] T. Huld et al. Mapping of photovoltaic module performance, effects of module type and part on Recovery, Util. Environ. Eff., 44 (3)

[19] C. Baldus-Jeursen, A. Côté, T. Cerf, Y. Poissant Analysis of the performance and degradation of the life cycle of a photovoltaic module from a 23-year-old network in Quebec, Canada Renew. Energy, 174 (August 2021), pp. 547-556, 10.1016/j.renene.2021.04.013

[20] P. Rodrigo, E.F. Fernandez, F. Almonacid, P. J. Perez-Higueras A simple accurate model for calculating shading power losses in photovoltaic generators. 2013 Solar Energy, pp. 322-333

[21] D.C. Jordan, C. Deline, S.R. Kurtz, G.M. Kimball, M. Anderson Robust methodology and application for PV degradation IEEE J. Photovoltaics, 8 (2) (March 2018), pp. 525-531, 10.1109/JPHOTOV.2017.2779779

[22] Relative change and difference, Wikipedia. July 11, 2023. Accessed July 18, 2023.

[23] U. Bouaichi, et al. In situ assessment of early degradation of photovoltaic modules of various technologies under harsh climatic conditions: the case of Morocco. Renewable Energy, 143 (Dec. 2019), pp. 1500-1518, 10.1016/j.renene.2019.05.091

[24] D. H. Daher, M. Aghaei, D. A. Quansah, M. S. Adaramola, P. Parvin, and C. Ménézo, "Multifaceted degradation analysis of a photovoltaic plant after 9.5 years of operation in hot desert climatic conditions," Prog. Photovoltaics Res. Appl., vol. n/a, no. n/a, doi: 10.1002/pip.3694.

[25] I. Kaaya, K.-A. Weiß. Assessment of long-term photovoltaic yield prediction variations due to solar irradiance and module temperature. Proceedings of the ISES World Solar Congress 2021, virtual, International Solar Energy Society (2021), pp. 1-6, 10.18086/swc.2021.37.04

[26] M. Koehl, M. Heck, S. Le juge Wiesmeier Wirth Modeling of the nominal temperature of the operating cell as a function of external weather conditions Sol. Energy Mater. Sol. Cells, 95 (7) (July 2011), pp. 1638-1646, 10.1016/j.solmat.2011.01.020

[27] I. Kaaya, J. Ascencio-Vásquez, K.-A. Weiss, M. Topič Evaluation of uncertainties and variations in the degradation rates of photovoltaic modules and lifetime predictions using physical models Sol. Energy, 218 (April 2021), pp. 354-367, 10.1016/j.solener.2021.01.071

[28] I. Kaaya, D. Mansour, P. Gebhardt, K. Weiß, D. Philipp Modeling and validation of photovoltaic degradation under ultraviolet heat and humid conditions.

[29] M. H. Adnan, K. Ismail, M. Al-Jbori, Q. Matti, Roland Sheer, Ralph Gottschalg Analysis and prediction of the performance and reliability of PV modules installed in harsh climates: case study Iraq

[30] Adannou, H. A; Goni, S., Abderaman, M. B, Khayal, M .Y., Khamis, A. A., Aidara, M., Kharouna, T. and Beye, A. C. (2019). Influence of climate temperature on the valorization of dung-Wastewater Slaughterhouse Biogas in Two Regions: In Chad and Senegal. Natural Resources, 10, 81-95.

[31] BIANZEUBE TIKRI et al., Influence of Sahelian and Sudanian provenance on the physical and mechanical properties of Faidherbia albida wood from Chad. Wood Material Science and Engineering, 17 (6): 693-701.

[32] Arafat Ousman Bechir, Design and implementation of calibration standards for 120° 3-port devices. Doctoral thesis, University of Lyon, 2016.

[33] Un. Omazic et al. Relationship between the degradation of polymer components in a crystalline silicon photovoltaic module and climatic conditions: a literature review. Sol. Energy Mater. Sol. Cells (2019)

[34] Un. Marzo et al. Standard or local solar spectrum? Implications for studies on solar technologies in the Atacama Desert. Renew. Energy (2018)

[35] P. Ferrada et al. Physico-chemical characterization of soiling in photovoltaic installations in the arid areas of the Atacama Desert. Sol. Energy (2019)

311

312

313

314

315

316

317

318

319